Available online at www.sciencedirect.com
ScienceDirect
International Journal of Pharmaceutics 350 (2008) 272–278
INTERNATIONAL JOURNAL OF PHARMACEUTICS
www.elsevier.com/locate/ijpharm

High throughput methods to characterize protein permeation and release

Martinus A.H. Capelle, Robert Gurny, Tudor Arvinte *

Department of Pharmaceutics and Biopharmaceutics, School of Pharmaceutical Sciences, University of Geneva, University of Lausanne, CH-1211 Geneva 4, Switzerland

Received 7 June 2007; received in revised form 27 August 2007; accepted 3 September 2007
Available online 14 September 2007

Abstract

Spectroscopic methods have been developed to study protein permeation and release kinetics in multi-well plates. The permeation of bovine serum albumin (BSA) through a membrane, which separated a 96-well plate in two compartments, was characterized. A change in fluorescence intensity was measured corresponding to the permeation of BSA from one compartment to another. The permeation of BSA was influenced by the pore size and pore density size of the membrane. The multi-well plates were also used to study the release of a protein drug, hirudin, from an agar hydrogel. A hirudin formulation was mixed at 60 °C with liquid agar and the mixture turned to a gel by cooling at room temperature. The gel entrapping hirudin was formed inside the wells of a 96-well plate. On top of the 100 μl agar–hirudin gel a volume of 200 μl of 10 mM phosphate buffer pH 7.4, 140 mM NaCl was added. The release kinetics of hirudin from the gel were measured following the changes in the hirudin intrinsic tyrosine fluorescence. The release of hirudin over 12 h was measured at three positions: at the bottom of the agar gel, at the interface of the gel with the solution, and in the middle of the receiver solution. The data presented in this paper indicate that high throughput methods can be applied in the characterization of protein drug release from drug delivery systems using small sample volumes.

Keywords: Protein formulation; Drug release; Permeability; Hirudin; High throughput screening

1. Introduction

Biopharmaceuticals are generally developed as liquid or lyophilized formulations for parenteral injection. However, in certain cases incorporation of proteins such as potent growth factors, local drug delivery systems would be beneficial. Specific release characteristics can reduce systemic toxicity that can arise after parenteral administration. Improving patient convenience and compliance by modifying already approved protein therapeutics, such as insulin, human growth hormone, interferons and erythropoietin is another reason for developing novel protein delivery systems (Cleland et al., 2001).

The success of a biopharmaceutical drug depends on the formulation in which the stability and activity is maintained during preparation, shipping, long-term storage and delivery. An important step during the development of new biopharmaceutical drugs and dosage forms is to gain insight and understanding into the protein release and stability properties. Standard Pharmacopeia methods are lacking to characterize proteins before, during, and after release from semi-solid drug delivery systems such as gels (Jorgensen et al., 2006). In recent literature, the use of Fourier transform-infrared spectroscopy (Jorgensen et al., 2004), differential scanning calorimetry (Green et al., 1999) and fluorescence spectroscopy (Castelain and Genot, 1994) of proteins have been described.

In this article, two fluorescence spectroscopic methods are presented that can be used for the high throughput screening (HTS) of a large variety of delivery systems. Our first model was developed to determine in time, in 96-well plates the permeation of bovine serum albumin (BSA) from one compartment to another. This permeation study can be used for the characterization of protein bearing delivery systems that are either in solution or suspension. The well plates used for this assay were Millipore MultiScreen® microplates, which are generally used for predicting absorption of orally administered drugs, either with a cellular (Irvine et al., 1999; Artursson et al., 2001) or artificial membrane layer (Wohnsland and Faller, 2001; Di et al., 2003; Kansy et al., 2004) as barrier. The second model is based on a validated *in vitro* release method of depot formulations that was described by Gietz et al. (1998). Their model delivery system was composed

* Corresponding author. Tel.: +41 22 3796339; fax: +41 22 3796567.
E-mail address: Tudor.Arvinte@pharm.unige.ch (T. Arvinte).

0378-5173/$ – see front matter © 2007 Elsevier B.V. All rights reserved.
doi:10.1016/j.ijpharm.2007.09.007

of an agar gel with hirudin or Zn–hirudin incorporated and was tested with commercial insulin formulations. We adapted this hirudin–agar system from 5 ml vials to a 96-well plate format.

Two different proteins were used in the present study, bovine serum albumin and hirudin. BSA has a molecular weight of 66.3 kDa and contains two tryptophan residues that were used as fluorophores. Hirudin has a molecular weight of 6.9 kDa and contains 65 amino acids including two tyrosine residues. A recombinant hirudin, derived from yeast cells, was used. Hirudin is a potent anticoagulant, which was originally isolated from the saliva of the medicinal leech, *Hirudo medicinalis* (Deutsch et al., 1993). Hirudin or Revasc® is approved as a subcutaneous injection for the prevention of deep venous thrombosis in patients undergoing elective hip and knee replacement surgery.

Fluorescence microplate readers measure in general the front-face fluorescence, enabling measurements in turbid drug delivery systems, with sensitivities similar to conventional cuvette-based spectrofluorometers. The microplate reader had two optical devices and could focus the fluorescence at different heights inside the well from the top while simultaneously measuring the fluorescence from the bottom. The intrinsic fluorescence properties of the two tyrosine residues present in hirudin, and the two tryptophan residues in BSA, were determined in time inside the delivery system as well as in solution. The advantages of high throughput analysis of proteins in two compartments are discussed in reference to the development of protein formulations.

2. Methods and materials

2.1. Materials

Agar, sodium chloride, sodium phosphate monobasic, sodium phosphate dibasic (all chemicals were minimum 99% pure) and bovine serum albumin (BSA, fraction V, minimum 98% pure) were provided by Sigma–Aldrich (Sigma–Aldrich Chemie GmbH, Buchs, Switzerland). For the BSA permeation experiment, Millipore (Millipore AG, Billerica, MA, USA) provided transparent MultiScreen® 96-well plates containing 0.65 μm Durapore® poly(vinylidene difluoride) (PVDF) (MADV N65), 3.0 μm polycarbonate membranes (MAPBMN3) and teardrop-shaped transparent polystyrene acceptor 96-well plates (MAMCS96). The r-hirudin (variant HV1) was from Novartis (Novartis AG, Basel, Switzerland). UV transparent 96-well Costar® (#3635) Corning (Corning Inc., New York, USA) microplates were supplied by Vitaris (Vitaris SA, Baar, Switzerland). Greiner VIEWseals™ (Greiner Bio-One GmbH, Frickenhausen, Germany) were acquired from Huber & Co. (Reinach, Switzerland).

2.2. Permeation of BSA from one compartment to another

The bovine serum albumin was solubilized at room temperature in purified MilliQ™ Millipore water. 100 μl of a 4.0 mg/ml BSA solution was pipetted in either the bottom or top compartment of a MultiScreen® 96-well plate. The bottom compartment was a polystyrene plate that contained 96 tear-shaped wells. The top compartment consisted of 96 wells with individual 0.65 μm Durapore® PVDF membranes. The volume equilibrium between the two solutions in the top and bottom compartment was maintained with volumes of 100 and 170 μl, respectively. To the BSA solution in the bottom compartment, 70 μl of MilliQ™ Millipore water was added. The top compartment was placed on the bottom compartment seconds prior to the start of the kinetic spectroscopic measurements. The assembled MultiScreen®96-well plate was sealed with a Greiner Viewseal™.

The permeation of BSA from the top to the bottom compartment and vice versa was characterized using a Tecan Safire™ (Tecan Group Ltd., Männedorf, Switzerland) microplate reader. The intrinsic Trp fluorescence of BSA was measured from the top, since the plastic of the MultiScreen® acceptor plate adsorbed UV light. The fluorescence emission was measured at 345 nm after excitation at 280 nm using bandwidths for both excitation and emission of 7.5 nm. The fluorescence was measured every 30 s during 10 h at 25 °C. The BSA samples were in duplicate. The BSA concentration equilibrium is at 1.5 mg/ml of the BSA solutions that were initially either in the top or bottom compartments. To control the experimental conditions and the influence of protein fluorescence originating from beneath the membrane, 1.5 and 4.0 mg/ml BSA solutions were added to both compartments. However, the membrane present in the top compartment prevented light from the top to pass to the bottom, eliminating fluorescence emission from proteins that were beneath the membrane.

2.3. Preparation of hirudin–agar gel

The hirudin lyophilisate was reconstituted through an addition of phosphate buffered saline (PBS) pH 7.4. The hirudin–agar gel was prepared similarly to the validated method described by Gietz et al. (1998). The agar was solubilized under continuous stirring in purified MilliQ™ Millipore water at a temperature of 80 °C. Three hirudin solutions (1/5) were mixed with a warm 1% agar solution (4/5) at a temperature of 60 °C, resulting in hirudin concentrations in 0.8% agar of 0.40, 0.80 and 1.60 mg/ml. Immediately after sample preparation, 100 μl of the warm hirudin–agar solution was pipetted in a Corning Costar® 96-well plate and kept at room temperature for 3 h until rigidification was completed. Four replicates per sample were prepared. The fluorescence properties of the 100 μl hirudin–agar gels were characterized before, during and after addition of 200 μl 10 mM phosphate buffer pH 7.4, 140 mM NaCl (PBS). The 96-well plate was sealed with a Greiner Viewseal™ to avoid evaporation. Similarly to the permeation experiment, two layers were present in the 96-well plate: bottom layer containing hirudin–agar gel and a top layer containing the PBS solution.

2.4. Continuous characterization of hirudin–agar gel during in-vitro protein release

The intrinsic hirudin fluorescence was measured with a Tecan Safire™ (Tecan Group Ltd., Männedorf, Switzerland) microplate reader, which consisted of two double monochromators, xenon flashlamp and a photomultiplier detector. The

fluorescence emission was measured every 60 s at 305 nm after excitation at 274 nm using bandwidths for both excitation and emission of 12 nm. The hirudin release was characterized by measuring the fluorescence intensity over 18 h. The top optics of the microplate reader focused at different *Z*-heights inside the wells and the focusing height is independent of the *Z*-height. The *Z*-height equals the distance of the top optical focusing lens to the top of the 96-well plate. To measure deep inside a 96-well, the *Z*-height is small. An increased *Z*-height is applied when measuring in the middle or top part of the 96-well. The fluorescence was measured at the optimal *Z*-height, 4.1 mm, for the hirudin–agar gel without receiver solution and, at the optimal *Z*-height, 8.5 mm of this system after hirudin release. Schematic representations of these *Z*-heights in relation to a 96-well are included in Figs. 5–7.

3. Results

3.1. BSA permeation

In Figs. 1 and 2, schematic representations of a Millipore MultiScreen® assembly show the acceptor tray with a top compartment comprising of a filter. The light was focused in the middle of the top compartment by the optical system at a *Z*-height of 7.9 mm. The BSA present in either the top (#4) or bottom (#2) compartment permeated through the 0.65 μm PVDF membrane to the other compartment, resulting in a change in fluorescence intensity (Fig. 1). No differences were observed between the sample duplicates. During the first hour of kinetic measurements, some fluctuations were observed in the BSA fluorescence intensity signal for the samples that were in both compartments at concentration equilibrium (#3 and #5, Fig. 1). These fluctuations were still present after conditioning of the membrane with BSA or with buffer which would exclude protein adsorption to the membrane as the cause of these fluctuations.

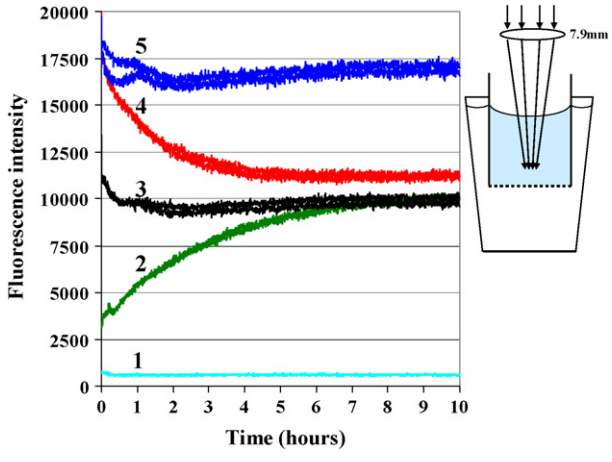

Fig. 1. The fluorescence intensity of BSA is measured in the top compartment, at a *Z*-height of 7.9 mm, of the assembled MultiScreen® microplate containing a 0.65 μm PVDF membrane. The fluorescence emission of BSA that permeated from the top compartment to the bottom is in red (#4) and the BSA that permeated from the bottom to the top compartment is in green (#2). BSA that is present at identical concentrations in both the top and bottom compartment is represented in black (#3) and blue (#5), 1.5 and 4.0 mg/ml, respectively. The control solutions with no BSA are depicted in turquoise (#1).

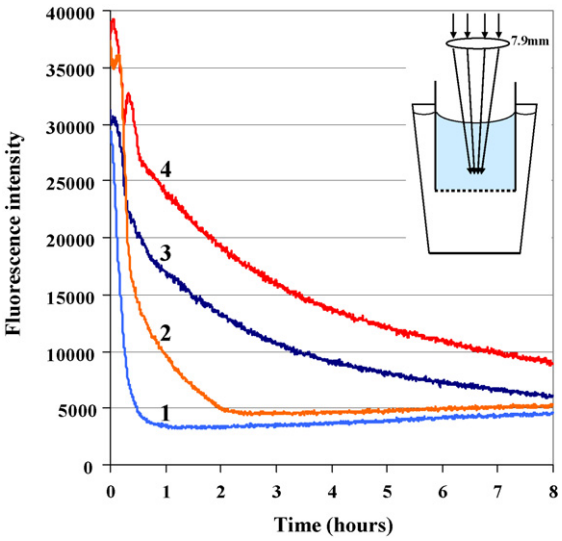

Fig. 2. The permeation of BSA from the top to the bottom compartment was characterized using two different membranes. The BSA solution was pipetted into the top compartment and permeated until concentration equilibrium was reached. The permeation of 0.6 mg/ml (#1, light blue) and 0.9 mg/ml (#2, orange) BSA through a 0.65 μm PVDF membrane was faster than the respective BSA permeation through a 3.0 μm polycarbonate membrane (#3, dark blue and #4, red).

The fluorescence intensities of the BSA samples that were initially in one compartment are not mirror images. The fluorescence intensity of BSA that was in the top compartment (#4) decreased faster in the first 4 h then the increase of the BSA that was pipetted in the bottom compartment (#2). The steady-state between the two compartments was reached for the BSA that was initially present in the top compartment (#4) after about 5 h, which is faster then the 7–8 h required for BSA initially present in the bottom compartment (#2). The small difference between the permeation profiles might be related to the different volumes present in the bottom and top compartment.

In another experiment, the permeation of BSA through two different membranes, a 0.65 μm PVDF and a 3 μm polycarbonate, was compared (Fig. 2). The permeation kinetics of BSA from the top compartment through the membrane and into the bottom compartment was monitored by a decrease in fluorescence intensity. The permeation of 0.60 and 0.90 mg/ml BSA solutions was faster when using a PVDF membrane with a pore size of 0.65 μm than with a polycarbonate membrane and pore size of 3.0 μm. The time to reach concentration equilibrium between the two compartments was faster for 0.60 mg/ml BSA than 0.90 mg/ml BSA. Scanning electron microscope images of a polycarbonate (Fig. 3A and B) and PVDF (Fig. 3C and D) membranes show the differences in structure. The active surface area, defined as membrane area × porosity, was 0.24 cm^2 × 20% = 0.048 cm^2 for the polycarbonate membrane and 0.24 cm^2 × 100% = 0.24 cm^2 for the PVDF membrane. Compared to the polycarbonate membrane, PVDF had a higher porosity and active surface area which resulted in faster BSA permeation.

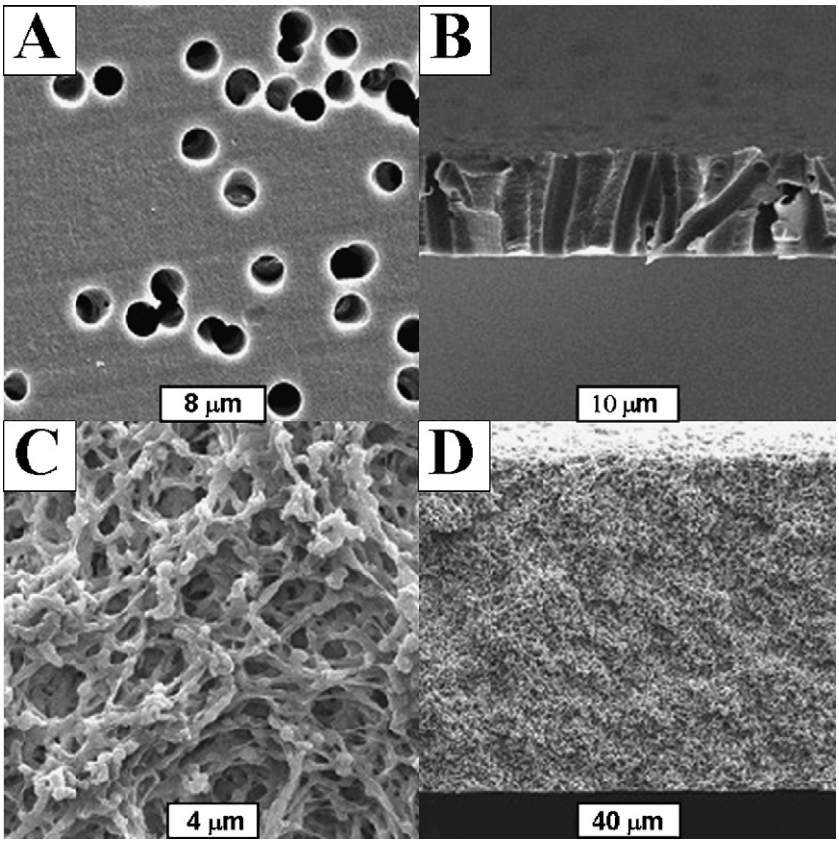

Fig. 3. Scanning electron microscope images are shown of a 0.4 μm polycarbonate (A, top view and B, cross-section) and a 0.45 μm PVDF membrane (C, top view and D, cross-section), courtesy of Millipore Corporation. The PVDF membrane has, compared to the polycarbonate membrane, a higher porosity density and active surface. Similar differences exist between the 3.0 μm polycarbonate and 0.65 μm PVDF membrane.

3.2. Hirudin release

The kinetics of hirudin release from a hydrogel was characterized in time by measuring the tyrosine fluorescence at three focal points inside the wells. The four sample replicates showed similar release profiles. In Table 1, the average fluorescence intensity values are shown of the agar gels with and without hirudin prior to addition of PBS solution to the hirudin–agar gel ($t = 0$ h), immediately after addition ($t = 0.2$ h) and after 18 h of hirudin release. The addition of PBS receiver solution to the hirudin–agar gels did not change the fluorescence bottom intensity. However, the fluorescence intensities measured at the interface of the gel and solution ($Z = 4.1$ mm) decreased. The fluorescence intensities in the middle of the receiver solution ($Z = 8.5$ mm) increased.

The hirudin fluorescence intensities measured with the bottom optics decreased during 18 h (Table 1 and Fig. 4). The release of hirudin that was present at the bottom part of the hirudin–agar gel was a gradual process and no significant difference between the fluorescence before and after addition of PBS solution to the gel was observed (Table 1 and Fig. 4). Removal of PBS after hirudin release did not alter the fluorescence bottom inten-

Table 1
The average fluorescence intensities at three different time points are given

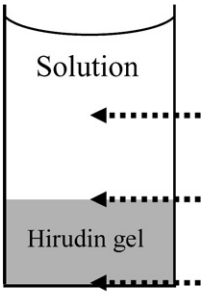

	Time	Hirudin in agar gel (mg/ml)			
	(h)	0	0.4	0.8	1.6
FI top	0	70	4,865	8,672	15,067
Z=8.5mm	0.2	3,440	9,700	14,711	22,073
	18	3,224	13,134	22,045	36,764
FI top	0	259	14,248	25,899	47,034
Z=4.1mm	0.2	1,136	7,074	12,678	20,265
	18	1,053	4,545	7,630	12,786
FI	0	362	14,775	27,308	50,228
Bottom	0.2	648	14,991	27,713	50,197
	18	545	7,095	13,032	24,593

At $t = 0$, the fluorescence was measured before an addition of receiver solution. At $t = 0.2$, the fluorescence emission was determined directly after the addition of PBS. At $t = 18$, the fluorescence intensity after 18 h of release is given. The fluorescence was determined at three Z-heights (schematic representation is on the left): centre of receiver solution ($Z = 8.5$ mm), interface solution and gel ($Z = 4.1$ mm) and inside gel (fluorescence bottom).

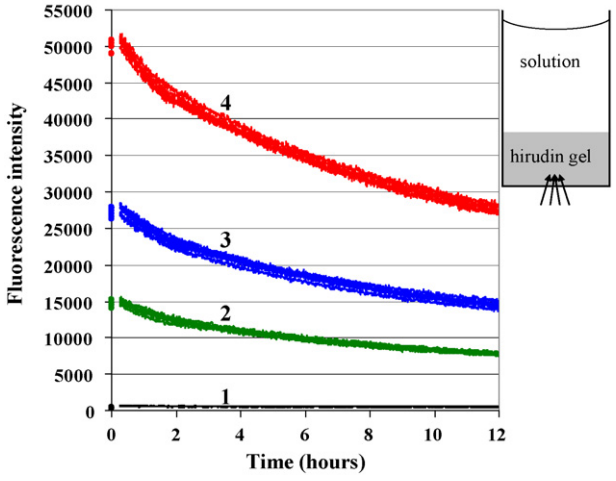

Fig. 4. The fluorescence emission from the bottom of the hirudin–agar gels containing no hirudin (#1, black), 0.40 mg/ml (#2, green), 0.80 mg/ml (#3, blue) and 1.60 mg/ml (#4, red) hirudin during more than 12 h are shown. The measurement at time 0 corresponds to the fluorescence prior to the addition of PBS.

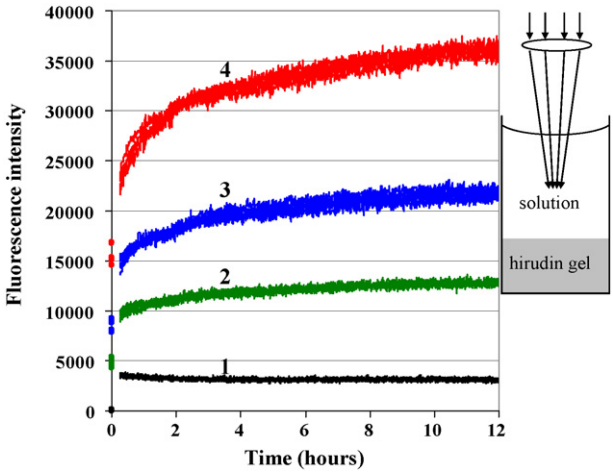

Fig. 6. The fluorescence emission from the top, at a *Z*-height of 8.5 mm, of the hirudin–agar gels containing no hirudin (#1, black), 0.40 mg/ml (#2, green), 0.80 mg/ml (#3, blue) and 1.60 mg/ml (#4, red) hirudin during 12 h is shown.

sity indicating that only hirudin inside the gel attributed to the measured intensity.

Figs. 5 and 6 show the two *Z* heights of the top optics and their respective focal points in solution ($Z = 8.5$ mm) and on top of the hirudin–agar gel ($Z = 4.1$ mm). The fluorescence at a *Z*-height of 4.1 mm was focused at the gel–solution interface, and decreased more than 50% after addition of PBS solution (Table 1). During the first 2 h after addition of PBS, a further burst release of hirudin was measured followed by a constant release over 10 h (Table 1 and Fig. 5).

The fluorescence measured in the centre of the PBS solution increased during the first 2 h followed by a slower continuous increase over the remaining 10 h (Table 1 and Fig. 6). An increase in fluorescence intensity was measured for all samples, including the control solutions, after the addition of PBS. This increase in signal from the control wells can be attributed to an increased reflection and light scatter. The increase in fluorescence intensity that occurred after addition of PBS receiver solution for the agar gels containing hirudin approximated those of the control agar gel (Table 1). The remaining difference in fluorescence signal was probably due to a burst release of hirudin, which occurred immediately after preparation and before the start of the analysis.

The fluorescence emission spectra were also determined before and after protein release to study possible changes in conformation. No shift in fluorescence emission maxima was measured from the bottom of the hirudin gel before and 18 h after addition of PBS (Fig. 7). This indicates that the local tyrosine environment of hirudin before and after release remained the same. The lower fluorescence intensities corresponded to the decrease in incorporated hirudin concentrations.

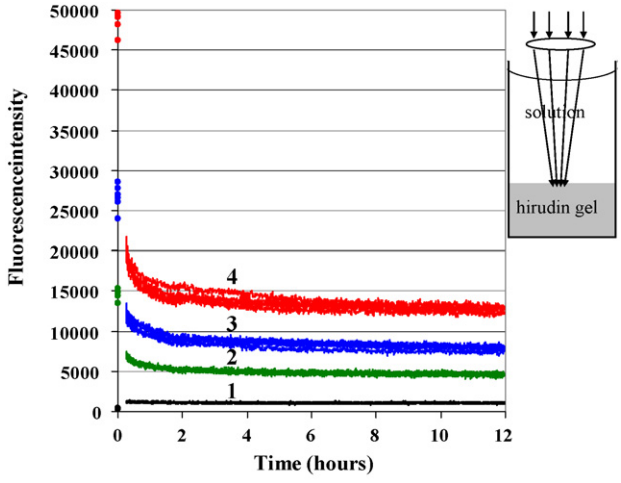

Fig. 5. The fluorescence emission from the top, at a *Z*-height of 4.1 mm, of the hirudin–agar gels containing no hirudin (#1, black), 0.40 mg/ml (#2, green), 0.80 mg/ml (#3, blue) and 1.60 mg/ml (#4, red) hirudin during 12 h is shown.

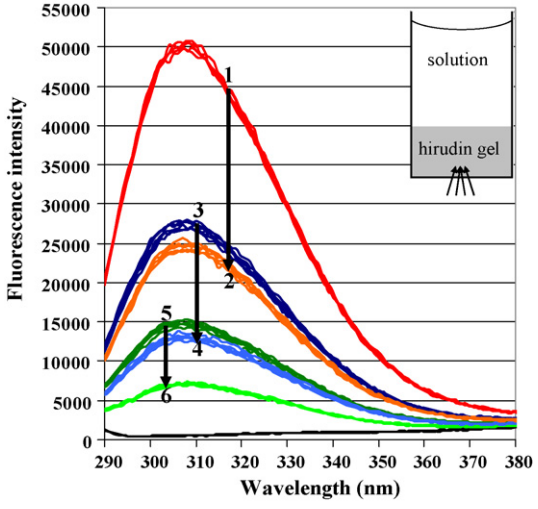

Fig. 7. The hirudin fluorescence emission spectra in agar were measured before the addition of PBS and after 18 h of protein release. The spectra of the hirudin gels containing 1.60, 0.80 and 0.40 mg/ml hirudin measured before and after release are depicted in red and orange (#1 and #2), dark blue and light blue (#3 and #4) and dark green and light green (#5 and #6), respectively. The wavelength with the maximum fluorescence emission was for all samples determined at 305 nm.

Table 2
The expected and measured hirudin concentrations that are remaining in the agar gel, as measured from the bottom, are shown

Concentration (mg/ml) at $t = 0$	Concentration (mg/ml) expected in equilibrium	Concentration (mg/ml) measured at $t = 18$ h
0.40	0.13	0.13
0.80	0.27	0.33
1.60	0.53	0.72

The initial highest concentration of hirudin in the gel had after 18 h of release still an excess of protein.

An estimation of the hirudin concentrations remaining inside the gel after 18 h was performed. The samples containing before release 0.40, 0.80 and 1.60 mg/ml hirudin in 100 μl agar had about 0.13, 0.33 and 0.72 mg/ml remaining after 18 h of release, respectively (Table 2). The results for the two lowest initial hirudin concentrations were similar to the expected concentrations in equilibrated state (Table 2). However, the hirudin at the highest initial concentration had not reached its concentration equilibrium, and an excess of hirudin remained in the gel. Removal of PBS solution from the samples and replacing with fresh buffer resulted in a further increased release of hirudin (data not shown). In another experiment, hirudin solutions were pipetted on top of an unloaded agar gel. The diffusion of hirudin into the gel was similar (data not shown) to the obtained release profiles.

4. Discussion

4.1. Permeation characterization

The fluorescence kinetics that were determined in the top compartment corresponded to the permeation of BSA through a membrane. No fluorescence was measured in the bottom compartment of the assembled MultiScreen® microplate. Development of UV transparent acceptor plates would make simultaneous intrinsic protein fluorescence detection in two compartments feasible. The continuous determination of the BSA permeation kinetics in well plates can complement established permeability assays such as the parallel artificial membrane permeability assay (PAMPA) (Kansy et al., 1998; Wohnsland and Faller, 2001), blood–brain barrier PAMPA (Di et al., 2003), Caco-2 cell monolayers (Artursson et al., 2001) and Madin–Darby Canine Kidney (MDCK) cells (Irvine et al., 1999). Other applications can be the determination in well plates of dissolution and solubility profiles of drugs and solid dosage forms. The solubilized compounds permeate through the membrane and are detected by fluorescence. Another possible application is the characterization of protein release from micro- or nanoparticulate drug delivery systems. The membrane blocks the drug delivery system but permits the diffusion of the active compound.

Both cellular assays and artificial membrane assays have in common that after incubation, the concentration of the permeated substance is measured in the top or bottom compartment or in both. Often a certain volume, e.g. 100 μl, is transferred to a second microplate before measuring the concentration by absorbance or fluorescence. Direct measurements inside the assembled microplates would reduce consumable costs and eliminate possible errors due to extra sample handling and analysis. The only prerequisite for a continuous permeation characterization is that the compounds fluoresce. A disadvantage of a detailed kinetic permeation study is the need for powerful data analysis tools due to the large amount of data points.

A wide variety of well plates are available with different material properties, number of wells, diameter, volume, height and color. The cellular permeation assays use either single or multiwell inserts, e.g. Transwell® from Corning, on which the cell layers are grown. Several companies, such as Millipore, Becton Dickinson, Greiner and Corning, have developed a wide variety of special microplates that contain two compartments. The choice of the correct membrane, material pore size and porosity influence the permeation as observed by comparing the BSA permeation through the PVDF and polycarbonate membrane (Figs. 2 and 3).

4.2. Protein release

A fast understanding of the protein release characteristics from drug delivery systems was achieved by using small sample amounts in 96-well plates. Other advantages are the possibility to compare simultaneously a variety of criteria such as receiver solutions, pH, temperature, drug loading and type of delivery system.

The release of hirudin from an agar hydrogel was characterized in time using intrinsic fluorescence spectroscopy. The decrease in time in the fluorescence intensity measured from the bottom corresponded to the hirudin release from the gel. Fluorescence measurements from the top enabled the characterization at the interface of the gel with the solution and in the centre of the solution. The time-dependent increase in fluorescence intensity in the centre of solution corresponded to the release of hirudin. The fluorescence detection from the bottom measured only the hirudin which was inside the agar gel. However, the fluorescence intensity measured with the top optics contained some fluorescence originating from the hirudin in the gel. The measured top fluorescence intensity had contributions of the molecules around the focal point. The use of a membrane for separating the compartments can eliminate possible interference from the bottom compartment.

Our new approach to study protein release and permeation kinetics can contribute to the present repertoire of high throughput methods for the characterization of physical and chemical properties of proteins (Capelle et al., 2007). The kinetic methods described in this paper could be used for the characterization of a broad variety of drug delivery systems, such as crystals (Jen et al., 2002), *in situ* forming hydrogels and implants (Ruel-Gariepy and Leroux, 2004), emulsions (Jorgensen et al., 2004) and suspensions. Possible conformational changes occurring in a delivery system could be detected by fluorescence and UV-vis absorbance spectroscopy. Aggregation of proteins inside or outside the delivery system can be detected by changes in turbidity (Eckhardt et al., 1994). A reduction in turbidity is expected when drugs are solubilized after release, e.g. crystals (Jen et al., 2002).

5. Conclusion

A high throughput 96-well plate system to study protein release and permeation from one compartment to another is described. The major advantages of using 96-well plates are the small sample amounts required, the gain of time and continuous kinetic characterization of multiple parameters. This system can in all likelihood be used for the development of a variety of semi-solid or solubilized drug delivery systems. The only requirement is the presence of a barrier between the compartments. In our case, the barrier consisted of a filter (BSA permeation) and of a delivery system (hirudin gel). Other possible pharmaceutical applications that can also be considered are: permeability screening through cellular (Caco-2, MDCK) or artificial membranes (PAMPA, BBB-PAMPA), *in situ* forming delivery systems, micro or nanoparticulate systems, turbid drug delivery systems, dissolution and solubilization assays, sedimentation studies and stability screening of emulsions and suspensions. Simultaneous fluorescence measurements at multiple positions inside and outside of a drug delivery system can offer new insights in the release and permeation characteristics of drugs.

Acknowledgements

We would like to thank Dr. Gertrud Beterams of Millipore Corporation for providing the MultiScreen® microplates and the scanning electron images of the PVDF and polycarbonate membranes.

References

Artursson, P., Palm, K., Luthman, K., 2001. Caco-2 monolayers in experimental and theoretical predictions of drug transport. Adv. Drug Deliv. Rev. 46, 27–43.

Capelle, M.A.H., Gurny, R., Arvinte, T., 2007. High throughput screening of protein formulation stability: practical considerations. Eur. J. Pharm. Biopharm. 65, 131–148.

Castelain, C., Genot, C., 1994. Conformational changes of bovine serum albumin upon its adsorption in dodecane-in-water emulsions as revealed by front-face steady-state fluorescence. Biochim. Biophys. Acta – Gen. Sub. 1199, 59–64.

Cleland, J.L., Daugherty, A., Mrsny, R., 2001. Emerging protein delivery methods. Curr. Opin. Biotechnol. 12, 212–219.

Deutsch, E., Rao, A.K., Colman, R.W., 1993. Selective thrombin inhibitors: the next generation of anticoagulants. J. Am. Coll. Cardiol. 22, 1089–1092.

Di, L., Kerns, E.H., Fan, K., McConnell, O.J., Carter, G.T., 2003. High throughput artificial membrane permeability assay for blood–brain barrier. Eur. J. Med. Chem. 38, 223–232.

Eckhardt, B.M., Oeswein, J.Q., Yeung, D.A., Milby, T.D., Bewley, T.A., 1994. A turbidimetric method to determine visual appearance of protein solutions. J. Pharm. Sci. Technol. 48, 64–70.

Gietz, U., Arvinte, T., Mader, E., Oroszlan, P., Merkle, H.P., 1998. Sustained release of injectable zinc-recombinant hirudin suspensions: development and validation of *in vitro* release model. Eur. J. Pharm. Biopharm. 45, 259–264.

Green, R.J., Hopkinson, I., Jones, R.A.L., 1999. Unfolding and intermolecular association in globular proteins adsorbed at interfaces. Langmuir 15, 5102–5110.

Irvine, J.D., Takahashi, L., Lockhart, K., Cheong, J., Tolan, J.W., Selick, H.E., Grove, J.R., 1999. MDCK (Madin–Darby canine kidney) cells: a tool for membrane permeability screening. J. Pharm. Sci. 88, 28–33.

Jen, A., Madorin, K., Vosbeck, K., Arvinte, T., Merkle, H.P., 2002. Transforming growth factor beta-3 crystals as reservoirs for slow release of active TGF-beta3. J. Control Release 78, 25–34.

Jorgensen, L., Moeller, E.H., van de, W.M., Nielsen, H.M., Frokjaer, S., 2006. Preparing and evaluating delivery systems for proteins. Eur. J. Pharm. Sci. 29, 174–182.

Jorgensen, L., van de, W.M., Vermehren, C., Bjerregaard, S., Frokjaer, S., 2004. Probing structural changes of proteins incorporated into water-in-oil emulsions. J. Pharm. Sci. 93, 1847–1859.

Kansy, M., Avdeef, A., Fischer, H., 2004. Advances in screening for membrane permeability: high-resolution PAMPA for medicinal chemists. Drug Discov. Today: Technol. 1, 349–355.

Kansy, M., Senner, F., Gubernator, K., 1998. Physicochemical high throughput screening: parallel artificial membrane permeation assay in the description of passive absorption processes. J. Med. Chem. 41, 1007–1010.

Ruel-Gariepy, E., Leroux, J.C., 2004. *In situ*-forming hydrogels—review of temperature-sensitive systems. Eur. J. Pharm. Biopharm. 58, 409–426.

Wohnsland, F., Faller, B., 2001. High-throughput permeability pH profile and high-throughput alkane/water log P with artificial membranes. J. Med. Chem. 44, 923–930.